

---

Garreht Quandt-Wiese

# Can the study of reduction probabilities reveal news about the nature of quantum state reduction?

**Abstract** A phenomenological model for the calculation of reduction probabilities of a superposition of several states is presented. The approach bases only the idea that quantum state reduction has its origin in a mutual physical interaction between the states. The model is explicitly worked out for the gravitational reduction hypothesis of Diósi and Penrose. It agrees for typical quantum mechanical experiments with the projection postulate and predicts regimes in which other behavior could be observed. An outlook is given, how the new effects can possibly become of interest for biology. For verification a feasible quantum optical experiment is proposed. The consequences of the approach are discussed. It is shown that any deviant behavior from the projection postulate comes in conflict with superluminal signaling.

**Keywords** quantum state reduction · projection postulate · gravity-induced wave-function collapse · superluminal signaling · quantum effects in biology

## 1 Introduction

A fundamental issue of quantum theory is the question about the reduction of the state-vector, also known as the collapse of the wave-function. A key problem for establishing a theory of quantum state reduction is the difficulty to get experimental facts for developing and verifying a theoretical approach. Our experimental knowledge about quantum state reduction might be characterized by the following issues:

1. The measurement process forces a reduction of the state-vector towards an eigenvector of the operator describing the measurement process.
2. The reduction probabilities towards these eigenvectors are given by the projection postulate [1].
3. The nonlocal nature of quantum state reduction is demonstrated by Bell-type experiments [2].

The question how much mass can be involved in a superposition before it decays by state reduction is so far open. A main problem is to distinguish the real reduction phenomenon from decoherence. A lower limit how much mass can be involved in a superposition can be estimated from recent experiments demonstrating e.g. quantum superpositions of fullerenes [3] or superconducting currents [4]. Due to the rare experimental facts about quantum state reduction a variety of different theoretical approaches were developed in the last decades. Several of them try to explain state reduction by physical mechanisms like

---

G. Quandt-Wiese  
Schlesierstr. 16  
64297 Darmstadt  
Germany  
E-mail: garreht.quandt-wiese@arcor.de

e.g. uncertainties of the space-time [5,6,7]. Others, as the GRW approach, introduce a spontaneous localization process, without having a concrete physical mechanism in mind [8,9]. Parallel to the theoretical activities a lot of experimental proposals were developed benefiting from recent technological progress [10,11,12,13,14,15,16,17,18,19,20,21]. But with none of them it was so far possible to bring more light into the subject.

The concern of this work is to stimulate the research of quantum state reduction by proposing new experiments. This is done by investigating the idea that state reduction has its origin in a somehow mutual physical interaction between the states of the superposition. The investigation is done with help of a phenomenological model, which aims at the calculation of reduction probabilities. The model's approach is to calibrate it for superposition of two states to the projection postulate and then to study its behavior for superpositions of more states. Although the model is explicitly worked out for the Diósi-Penrose approach of gravity-induced quantum state reduction, other approaches for the physical interaction between the states can be plugged into the model as well.

In Chapter 2 the phenomenological model is introduced and the Diósi-Penrose approach of gravity-induced quantum state reduction is recapitulated. The application of the phenomenological model to thought experiments predicts regimes, in which deviant behavior from the projection postulate could be observed. In Chapter 3 the question is discussed whether the model can explain the reduction behavior of typical quantum mechanical experiments, in which deviations from the projection postulate are not observed so far. This discussion is based on an analysis of the decay behavior of solid states in a quantum superposition. In Chapter 4 the question is followed up whether it is possible to verify the predictions of the model with current state of the art technology. This is done by proposing and analyzing a concrete quantum optical experiment. Chapter 5 gives an outlook on the possible role of quantum state reduction in biology. Finally the approach is analyzed from the view point of quantum non-locality in concrete its consequences for signaling.

## 2 Model

In the derivation of the following phenomenological model it is assumed that according to Penrose [7, 22] state evolution can be described by a formal sequence of U- and R-processes, where the U-process is the unitary evolution of the state vector, described e.g. by the Schrödinger equation, and the R-process is causing the reduction of the state vector. Furthermore, it is assumed that there exists a statistical process, which triggers the R-processes on quantum superpositions. This process shall be denoted here as the "reduction triggering process". The lifetimes of quantum superpositions, predicted e.g. by the Diósi-Penrose approach, are correlated to this process in the following way. The life-time  $\tau$  corresponds to a decay rate  $\dot{p}_{decay}$  by  $\dot{p}_{decay} = 1/\tau$ , where the decay rate  $\dot{p}_{decay}$  describes the probability  $\Delta p$  that the reduction triggering process triggers within a given time-interval  $\Delta t$  an R-process ( $\dot{p}_{decay} = \Delta p/\Delta t$ ). In the Diósi-Penrose approach the derived decay rate does not distinguish, whether the superposition decays towards state 1 or 2. The basic idea of the following phenomenological model is to introduce a "direction" for the reduction triggering process, i.e. to write down separate trigger rates for stimulating a decay of state 1 towards state 2 ( $\dot{p}_{decay}^{1 \rightarrow 2}$ ) and vice versa ( $\dot{p}_{decay}^{2 \rightarrow 1}$ ). But before developing the model in detail, the basics of the Diósi-Penrose approach shall be recapitulated.

In the derivation of Penrose the hypothesis of gravity-induced quantum state reduction is a manifestation of the incompatibility of general relativity and the unitary time evolution of quantum physics [7, 22]. Penrose's basic idea can be explained with the thought experiment shown in Figure 1. Depending on whether the diffracted photon is detected by the detector at the right, a rigid mass inside the detector is shifted by a small distance or not. Following the unitary evolution of the Schrödinger equation the system evolves at this experiment into a superposition of two macroscopic states corresponding to the shifted and not shifted mass. According to the theory of general relativity the superposed macroscopic states have slightly different space-time geometries, which means that a clock at the same position runs with slightly different speeds. Penrose argues that due to this the time-translation operator for the superposed space-times involves an inherent ill-definedness leading to an essential uncertainty in the energy of the superposed states, which results finally to a decay of the superposition towards to

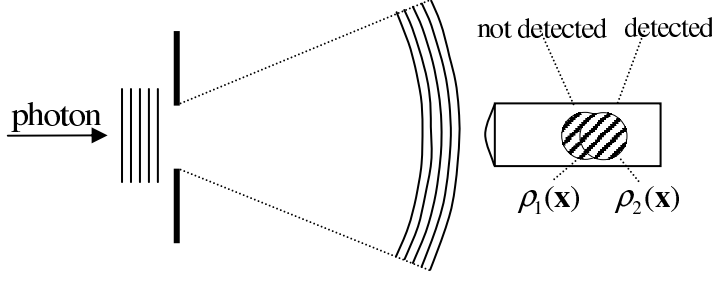


**Fig. 1** Thought experiment for generating a quantum superposition of a macroscopic rigid mass at two different locations. If the diffracted photon is measured by the detector, the position of the mass is shifted by a small distance.

one of the states. The expression

$$E_{G1,2} = \xi G \int d^3\mathbf{x} d^3\mathbf{y} \frac{(\rho_1(\mathbf{x}) - \rho_2(\mathbf{x}))(\rho_1(\mathbf{y}) - \rho_2(\mathbf{y}))}{|\mathbf{x} - \mathbf{y}|} \quad (1)$$

( $G$  =gravitational constant,  $\rho_i(\mathbf{x})$  =mass-density distribution of state  $i$ ,  $\xi$  dimensionless parameter, which is expected to be in the order of  $1^1$  [11]) defines a measure how much the space-time geometries of the states 1 and 2 differ from each other [6,7,23]. If the superposition consists of a rigid mass at different locations, equation (1) expresses the mechanical work, which is needed to separate the masses from each other under the assumption that gravitation acts between them. The stability of the superposition is expressed by the decay rate

$$\dot{p}_{decay} = \frac{E_{G1,2}}{\hbar} \quad (2)$$

or its corresponding lifetime  $\tau = 1/\dot{p}_{decay}$ . A derivation of equations 1 and 2 basing on the argumentation above is given in Appendix A.

For superpositions of atoms and molecules the Diósi-Penrose hypothesis predicts in consistency to quantum theory extremely long life-times. Lifetimes in the order of seconds are predicted for masses and lengths in the order of the bacterial scale (microns). With current state of the art technology it was so far not possible to study the decay of quantum superpositions involving masses of this order. Concrete proposals for checking the Diósi-Penrose hypothesis were developed by several authors [10, 11, 12, 13].

In the following discussion of the phenomenological reduction model a special representation for the wave-function is used, which is shown in Figure 2: This figure shows schematically the distribution of the wave-function in configuration space for experiment 1 shortly after the photon has reached the detector. The wave-function  $\Psi_{System}$  describes here always the whole system consisting in the experiment of Figure 1 of photon, aperture and detector. The configuration space on which the wave-function  $\Psi_{System}$  is defined is given for a many particle system mainly by the positions of all participating particles ( $\mathbf{x}_1, \dots, \mathbf{x}_n$ ).

The configuration space shall always be chosen in such a way that a classical state corresponds to a wave-function  $\Psi_{System}$ , which is localized around one point in the space. The quantum superposition evolving at the experiment of Figure 1 is then represented by a wave-function localized at two well distinguished points corresponding to the states "photon detected" and "photon not detected" respectively, as indicated at the right of Figure 2. Both axis of Figure 2 (and the following Figures 3, 8 and 9) represent the almost infinite dimensions of the configuration space. Since each point of the configuration space represents a classical state with a well defined mass-density distribution  $\rho(\mathbf{x})$ , expression  $E_{G1,2}$  (1) can be calculated for each pair of points in the configuration space as indicated in Figure 2 for state 1 and 2. By integrating  $|\Psi_{System}|^2$  in the surroundings of state 1 and 2 the amount of their amplitudes  $|c_i|^2$  can be defined as shown in Figure 2. For the state amplitudes  $|c_1|^2$  and  $|c_2|^2$  applies

<sup>1</sup> In all following calculations  $\xi$  is assumed to be 1.

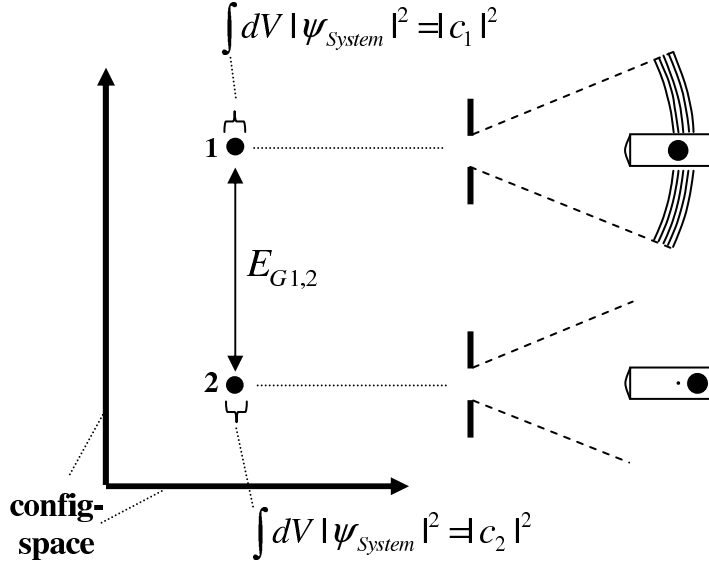


**Fig. 2** Distribution of the wave-functions ( $|\Psi_{System}|^2$ ) in configuration space for the experiment of Figure 1 shortly after the photon was detected. The wave-function is localized at two points corresponding to the states "photon detected" and "photon not detected".

the normalization  $|c_1|^2 + |c_2|^2 = 1$ . From the projection postulate the reduction probabilities towards state 1 and 2 are expected to be  $|c_1|^2$  and  $|c_2|^2$  respectively.

Let's now return to the derivation of the reduction model. The basic idea of the model is to split the decay rate (2) describing the probability for triggering an R-process into two rates specifying the direction of the decay like

$$\dot{p}_{decay} \Rightarrow \dot{p}_{trigger}^{1 \rightarrow 2} + \dot{p}_{trigger}^{2 \rightarrow 1} . \quad (3)$$

Under the assumption that the direction of the reduction triggering process determines the final outcome of the experiment, i.e. a triggering of a decay of state 1 towards state 2 ( $\dot{p}_{trigger}^{1 \rightarrow 2}$ ) leads finally to a complete vanishing of state 1 and a reduction towards state 2,  $\dot{p}_{trigger}^{1 \rightarrow 2}$  and  $\dot{p}_{trigger}^{2 \rightarrow 1}$  have to be chosen like

$$\dot{p}_{trigger}^{1 \rightarrow 2} = \frac{E_{G1,2}}{\hbar} |c_2|^2, \quad \dot{p}_{trigger}^{2 \rightarrow 1} = \frac{E_{G1,2}}{\hbar} |c_1|^2 \quad (4)$$

to calibrate the model to the predictions of the projection postulate. For a quantum superposition of more than two states the trigger rates (4) can be generalized like

$$\hbar \dot{p}_{trigger}^{i \rightarrow j} = E_{G i,j} |c_j|^2, \quad (5)$$

where  $E_{G i,j}$  is the generalization of expression (1) for a pair of states  $i$  and  $j$ . Expression (5) is interpreted in the following as the probability rate for triggering a decay of state  $i$  towards state  $j$ .

Before calculating the final outcome of the experiment with expression (5), a physical interpretation of the chosen approach shall be presented: Summing all trigger rates (5), which trigger the decay of a certain state  $i$ , one can define a decay rate for this state as<sup>2</sup>

$$\hbar \dot{p}_{decay}^i = \sum_{j \neq i} \hbar \dot{p}_{trigger}^{i \rightarrow j} = \sum_j E_{G i,j} |c_j|^2 . \quad (6)$$

<sup>2</sup> Note that the matrix  $E_{G i,j}$  is symmetrical ( $E_{G i,j} = E_{G j,i}$ ) and that its diagonal elements are vanishing  $E_{G i,i} = 0$ .

With the definition of the gravitational potential of a state  $i$

$$\phi_i(\mathbf{x}) = -G \int d^3\mathbf{y} \frac{\rho_i(\mathbf{y})}{|\mathbf{x} - \mathbf{y}|}, \quad (7)$$

and the normalization  $\sum_i |c_i|^2 = 1$ , equation (6) can be transformed to

$$\hbar \dot{p}_{decay}^i = \left( \int d^3\mathbf{x} \phi_{mean}(\mathbf{x}) \rho_i(\mathbf{x}) - \int d^3\mathbf{x} \phi_i(\mathbf{x}) \rho_i(\mathbf{x}) \right) + \left( \int d^3\mathbf{x} \phi_i(\mathbf{x}) \rho_{mean}(\mathbf{x}) - \sum_j |c_j|^2 \int d^3\mathbf{x} \phi_j(\mathbf{x}) \rho_j(\mathbf{x}) \right), \quad (8)$$

where the mean mass distribution and potential are defined by

$$\rho_{mean}(\mathbf{x}) = \sum_i |c_i|^2 \rho_i(\mathbf{x}), \quad \phi_{mean}(\mathbf{x}) = -G \sum_i |c_i|^2 \int d^3\mathbf{y} \frac{\rho_i(\mathbf{y})}{|\mathbf{x} - \mathbf{y}|}. \quad (9)$$

With the approximation that the gravitational self energies of the states are nearly identical ( $\int d^3\mathbf{x} \phi_i \rho_i \approx \int d^3\mathbf{x} \phi_j \rho_j$ ) expression (8) can be simplified to

$$\hbar \dot{p}_{decay}^i \approx 2 \left( \int d^3\mathbf{x} \phi_{mean}(\mathbf{x}) \rho_i(\mathbf{x}) - \int d^3\mathbf{x} \phi_i(\mathbf{x}) \rho_i(\mathbf{x}) \right). \quad (10)$$

This yields the physical interpretation that the decay rate of a state  $i$  is given by the energy difference of this state in the mean gravitational potential of the superposition and its own gravitational potential. For a superposition of two states, where  $|c_1|^2$  is much bigger than  $|c_2|^2$ , the mean potential is close to the potential of state 1 and its decay probability is small. For state 2 one gets a big energy difference and a high decay rate. Consequently the superposition mostly decays towards state 1.

Let's now continue with the calculation of the final outcome of the experiment. From the assumption that the reduction triggering process ( $\hbar \dot{p}_{trigger}^{i \rightarrow j} = E_{G_{i,j}} |c_j|^2$ ) induces a reduction stream from state  $i$  towards state  $j$ , which might be defined as  $J_{i \rightarrow j} = \frac{d}{dt} |c_j|^2 - \frac{d}{dt} |c_i|^2$ , it follows that the reduction streams of all other States  $k$  towards state  $j$  become also bigger than 0 ( $J_{k \rightarrow i} > 0$ ), since  $\frac{d}{dt} |c_j|^2$  is bigger than 0 and  $\frac{d}{dt} |c_k|^2$  equals 0. Since there is a physical interaction between these states described by the matrix element  $E_{G_{i,j}}$ , it is assumed that this net stream from state  $k$  towards state  $j$  triggers like the reduction triggering process  $\hbar \dot{p}_{trigger}^{k \rightarrow j}$  a reduction stream from state  $k$  towards state  $j$ . This means that the initial trigger event determines the final outcome of the experiment<sup>3</sup>. By summing up all trigger rates towards a state  $j$  one can define a reduction rate for this state describing all trigger events leading to a reduction towards this state like

$$\hbar \dot{p}_{reduce}^j = \sum_{i \neq j} \hbar \dot{p}_{trigger}^{i \rightarrow j} = \left( \sum_i E_{G_{i,j}} \right) |c_j|^2. \quad (11)$$

By summing up all scenarios, which lead finally to a reduction towards state  $j$ , the reduction probability  $p_j$  can be calculated like

$$p_j = \int_{t_0}^{\infty} p_{sup\ stable}(t) \dot{p}_{reduce}^j(t) dt; \quad p_{sup\ stable} = e^{-\int_{t_0}^t dt \sum_i \dot{p}_{decay}^i(t)}, \quad (12)$$

---

<sup>3</sup> This assumption loses its validity, if one regards for one amplitude of a superposition the limiting case  $|c_i|^2 \rightarrow 0$ . Here the reduction stream  $J_{i \rightarrow j}$  becomes so small that later occurring trigger events can overrule the final outcome of the experiment. This problem of the draft estimations (12) and (13) can be seen, if one studies the transition of a superposition of three states towards a superposition of two states by choosing  $|c_i|^2 \rightarrow 0$ . Here one will find discontinuities of the reduction probabilities as a function of  $|c_i|^2$  at  $|c_i|^2 = 0$ . But to get a first understanding of the model this effect can be neglected.

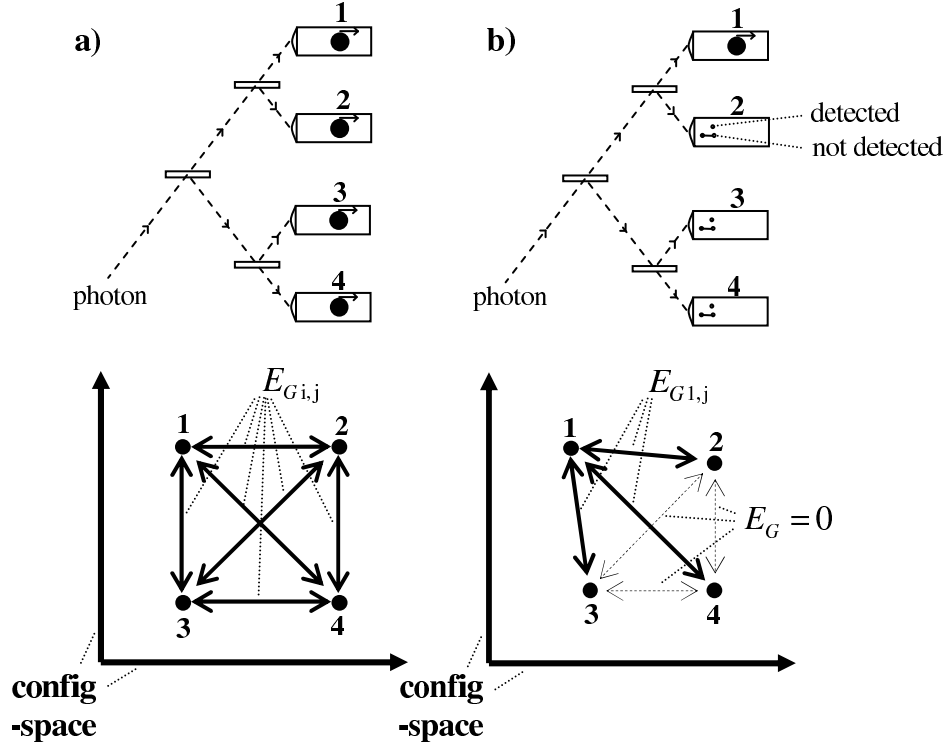


**Fig. 3** Comparison of two thought experiments generating superpositions of four macroscopic states. At experiment b) the three lower detectors of experiment a) are replaced by MDD conserving detectors, which leads to a changed concurrency situation between the states, as indicated at the lower part of the figure.

where  $p_{sup\ stable}(t)$  is the probability that the quantum superposition stays stable till the time  $t$  and  $t_0$  is the time, when the states of the superposition start to separate from each other. If the time dependencies of all couplings  $E_{G i,j}(t)$  are equal, the calculation of equation (12) simplifies to

$$p_j \propto \left( \sum_i E_{G i,j} \right) |c_j|^2, \quad (13)$$

where the proportional constant of equation (13) can be determined with the normalization  $\sum_j p_j = 1$ .

An important property of the derived model is that the predicted reduction probabilities do not depend on the coherence of the superposed states since  $p_j$  in equation (13) depends only on the amounts of the state amplitudes  $|c_j|^2$ . A more general argument for the independence of the reduction behavior from decoherence is simply the fact that the Diósi-Penrose approach predicts state reduction in regimes, where coherence between the states is normally lost. Since reduction behavior according to the projection postulate takes place in a regime, where coherence is lost, it is obvious that reduction behavior different from the projection postulate (predicted by the model) is also not impacted by decoherence.

Let's now turn to the discussion of thought experiments. At the upper diagram of Figure 3a an experiment is shown, at which a single photon is split into four beams, where the photon is detected at each beam by the same kind of detector as in Figure 1. The matrix  $E_{G i,j}$  for this experiment is given by

$$E_{G i,j}(t) = \begin{bmatrix} 0 & 2E_G(t) & 2E_G(t) & 2E_G(t) \\ 2E_G(t) & 0 & 2E_G(t) & 2E_G(t) \\ 2E_G(t) & 2E_G(t) & 0 & 2E_G(t) \\ 2E_G(t) & 2E_G(t) & 2E_G(t) & 0 \end{bmatrix}, \quad (14)$$

where  $E_G(t)$  is the evaluation of  $E_{G1,2}$  (equation (1)) for a single detector between the states "photon detected" and "no photon detected".  $E_G(t)$  is zero when the photon enters the mirrors and arrives a constant value after the detector has shifted the position of its mass. By inserting matrix (14) into equation (13) one gets the reduction probabilities predicted by the projection postulate  $p_i = |c_i|^2$ . From equation (13) one can easily see that the projection postulate is always reproduced, if the couplings  $E_{G i,j}$  between the superposed states are all equal.

At Figure 3b the experiment of Figure 3a is modified. The three lower detectors are replaced by so called "mass-density distribution conserving detectors" (MDD conserving detector), which means that these detectors do not change their mass-density distributions during the detection process. But nevertheless these detectors shall store the information, whether a photon was detected or not, persistently, so that this information can be read after the decay of the superposition has taken place. This persistent storage of information inside the detector is indicated in Figure 3b by the switches, which can have the positions "detected" and "not detected". In Chapter 4 the question will be pursued whether it is possible to construct such a MDD conserving detector.

The matrix  $E_{G i,j}$  of the experiment of Figure 3b is given by

$$E_{G i,j}(t) = \begin{bmatrix} 0 & E_G(t) & E_G(t) & E_G(t) \\ E_G(t) & 0 & 0 & 0 \\ E_G(t) & 0 & 0 & 0 \\ E_G(t) & 0 & 0 & 0 \end{bmatrix}. \quad (15)$$

The difference between the coupling matrices of experiments 3a and 3b is visualized in the lower part of Figure 3, which shows that in experiment 3b there are no couplings between the states 2, 3 and 4 anymore ( $E_{G i,j} = 0$ ). With result (13) the probability for detecting the photon at detector 1 is obtained to be  $p_1 = 0.5$ , if the photon intensity is split symmetrically at the mirrors ( $|c_1|^2 = |c_2|^2 = \dots = 0.25$ ). For the other detectors one gets  $p_2 = p_3 = p_4 = \frac{1}{3} \cdot 0.5$ . But since the couplings between the states 2, 3 and 4 are zero ( $E_{G i,j} = 0$ ), it is expected that a triggering of a reduction event from state 1 towards e.g. state 2 causes no reduction stream from the other states 3 and 4 towards state 2. Furthermore, the initial reduction stream  $J_{1 \rightarrow 2}$  has the effect that  $J_{1 \rightarrow 3}$  and  $J_{1 \rightarrow 4}$  are also bigger than zero<sup>4</sup>, which induces a decay of state 1 towards the states 3 and 4 as well. The final result is therefore expected to be a superposition of the states 2, 3 and 4. The probability for this superposition is also 0.5 ( $p_{sup 2,3,4} = 0.5$ ). The deviation from the projection postulate for the reduction probability of state 1 (0.5 instead of 0.25) becomes more dramatic, if one evaluates an analogous experiment with 8 detectors, where seven of them are MDD conserving detectors. The reduction probability for state 1 is again 0.5. The same result is also obtained for experiments with 16, 32, 64 etc. detectors. This 50%-rule can also be seen directly from the structure of the couplings (Figure 3b). Here one has six non-vanishing trigger rates ( $\dot{p}_{trigger}^{2 \rightarrow 1}$ ,  $\dot{p}_{trigger}^{3 \rightarrow 1}$ ,  $\dot{p}_{trigger}^{4 \rightarrow 1}$ ,  $\dot{p}_{trigger}^{1 \rightarrow 2}$ ,  $\dot{p}_{trigger}^{1 \rightarrow 3}$ ,  $\dot{p}_{trigger}^{1 \rightarrow 4}$ ), which have all the same amount, and where half of them reduce the superposition towards state 1 and the other ones towards the superposition of the other states. This dramatic change in the reduction behavior provokes questions, which define the guideline of the following chapters.

1. Why have such significant effects not been observed so far? Or: How far is the proposed model consistent to known experimental results? This is the subject of the following chapter.
2. How can the predicted behavior of the reduction model been verified by experiments? This question is the subject of Chapter 4, in which a concrete experiment is proposed.
3. Does the dramatic increase of the reduction probability towards a distinguished state play a role in nature? This question is picked up in Chapter 5.

### 3 Discussion of standard quantum mechanical experiments

To get an understanding how the proposed reduction model behaves in typical quantum mechanical experiments it is necessary to understand the decay behavior of a solid state in a quantum superposition. Such a quantum superposition occurs e.g. in the experiment of Figure 1, where the mass inside

---

<sup>4</sup> From  $\frac{d}{dt}|c_1|^2 < 0$  and  $\frac{d}{dt}|c_3|^2 = \frac{d}{dt}|c_4|^2 = 0$  follows  $J_{1 \rightarrow 3} > 0$  and  $J_{1 \rightarrow 4} > 0$ .

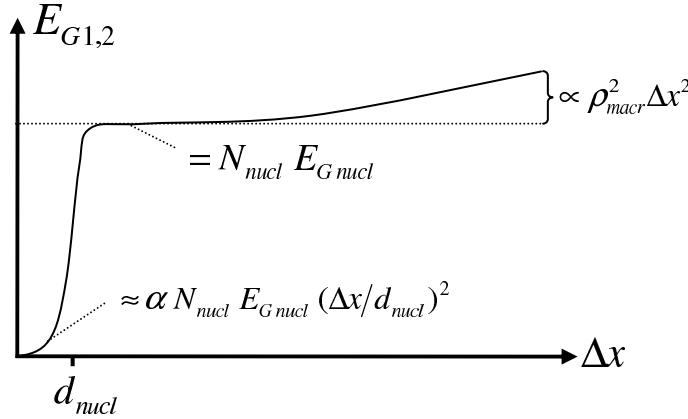


**Fig. 4** Dependency of  $E_{G1,2}$  for a superposed amorphous solid state on the displacement  $\Delta x$  between the two superposed states.

the detector is shifted by a small distance  $\Delta x$ , depending on whether the photon is detected or not. The vibration of the nuclei around their fix-positions in a solid state leads to a broadening of the extension of the wave-function  $\Psi_{System}$  in configuration space. At the application of the Diósi-Penrose approach the mass-density distribution  $\rho(\mathbf{x})$  in expression (1) has to be determined for the broadened wave-function  $\Psi_{System}$ . This means that the mass-density distribution  $\rho(\mathbf{x})$  is approximately given by Gaussian distributions around the fix positions of the nuclei, where the mean diameter for the extension of the nuclei  $d_{nucl}$  is mainly determined by acoustical phonons, which can be estimated with  $d_{nucl} \approx \sqrt{2kT/m_{nucl}(l_{lattice}/v_{phonon})}$  ( $k$  = Boltzmann constant,  $T$  = temperature,  $m_{nucl}$  = mass of nucleus,  $l_{lattice}$  = lattice constant,  $v_{phonon}$  = velocity of the acoustical phonons). For iron at room temperature  $d_{nucl}$  is roughly  $d_{nucl} \approx 0.2 \cdot 10^{-10}$  m. For an amorphous solid state it is expected that the quantity  $E_{G1,2}$  achieves a constant value after all its nuclei are separated far enough from each other, i.e. for  $\Delta x \gg d_{nucl}$ , as schematically shown in Figure 4. The amount of this value, which shall be denoted here as the microscopic contribution to  $E_{G1,2}$ , is given by the gravitational energy, which is needed to separate all the nuclei from each other<sup>5</sup>. The amount of the microscopic contribution is then just given by the number of nuclei  $N_{nucl}$  multiplied with the energy  $E_{G nucl}$  to bring a single nucleus in a quantum superposition of spatially far separated states

$$E_{Gi,j} = N_{nucl} E_{G nucl} . \quad (16)$$

With the approximation that the density distribution of one nucleus inside the sphere with diameter  $d_{nucl}$  is constant, the energy  $E_{G nucl}$  is given by

$$E_{G nucl} = \frac{12}{5} \frac{G m_{nucl}^2}{d_{nucl}} . \quad (17)$$

For 100 g iron at room temperature equation (16) predicts a decay rate of roughly  $E_{G1,2}/\hbar \approx 10^9 \text{s}^{-1}$ . For small displacements ( $\Delta x \ll d_{nucl}$ )  $E_{G1,2}$  scales with  $\Delta x$  like (see Figure 4)

$$E_{G1,2} \approx \alpha N_{nucl} E_{G nucl} (\Delta x/d_{nucl})^2 , \quad (18)$$

where  $\alpha$  is roughly 5. For bigger displacements ( $\Delta x \gg d_{nucl}$ ) a macroscopic contribution has to be added on top of the microscopic one, which has as its physical origin that the center of masses of both states are separated from each other. This contribution depends on the shape of the solid and the direction of the displacement. We give two examples: a) For a long rod with length  $l$  and diameter  $d$  ( $l \gg d$ ), which is displaced along its axis,  $E_{G1,2}$  scales for  $\Delta x \ll l$  like

$$E_{G1,2} \approx \beta G d^3 \rho_{macr}^2 \Delta x^2 \quad (19)$$

<sup>5</sup> Remember that equation (1) expresses for rigid masses the energy needed to separate the masses of the states against their gravitational attraction from each other.



( $\rho_{macr}$  = macroscopic averaged density of the solid), where  $\beta$  is approximately 5. b) For a disc ( $l \ll d$ )  $\beta$  becomes significantly lower and the result depends also on the ratio of  $l$  and  $d$ .

For a rod made of 100g iron ( $d = 1cm$ ,  $l \approx 16cm$ ) the macroscopic contribution (19) achieves the same decay rate as the microscopic one ( $E_{G1,2}/\hbar \approx 10^9 s^{-1}$ ) for a displacement of roughly  $\Delta x \approx 20 \cdot 10^{-10}m$ .

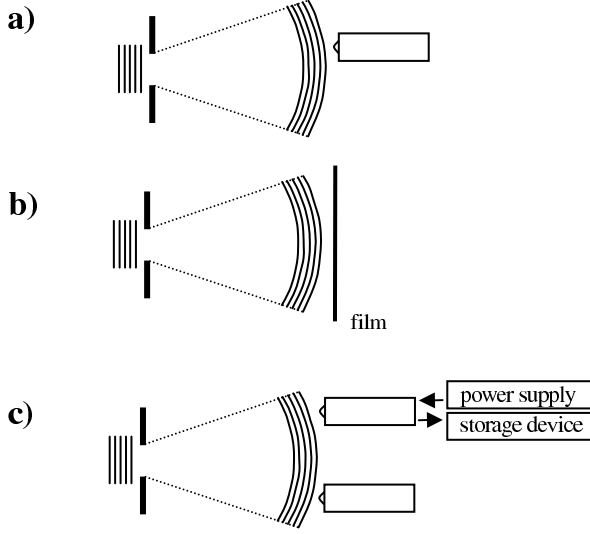


**Fig. 5** Three types of typical quantum mechanical experiments: a) Diffracted particle is detected by one detector. b) Particle is detected by a continuous medium. c) Particle is detected by two detectors simultaneously.

Let's now turn to the discussion of typical quantum mechanical experiments. In Figure 5 three different types of experiments are shown. In experiment a) the position of a diffracted particle is measured by a detector. According to the discussion of the experiment of Figure 1 the system turns here into a superposition of two states corresponding to the cases "particle detected" and "particle not detected", for which the reduction model reproduces per definition (its calibration) the projection postulate. In experiment b) the particle is detected by a continuous medium, a film. This case can be treated as follows. The continuous detection medium can be modeled by an infinite number of small detectors. In this case one gets an infinite number of superpositions and all off-diagonal elements of the matrix  $E_{G i,j}$  have the same amount, which leads according equation (13) to the reduction probabilities predicted by the projection postulate.

In experiment c) the particle is measured by two detectors simultaneously. Here one has a superposition of three states (state 1 = "particle detected at upper detector", state 2 = "particle detected at lower detector", state 3 = "particle not detected"). Since the matrix element  $E_{G1,2}$  is in this case twice as big as the other two couplings  $E_{G1,3}$  and  $E_{G2,3}$ , the observation of deviations from the projection postulate should be possible. But these deviations are difficult to observe: One reason is that the two detectors need a perfect synchronization in time. The discussion of the decay rates of superposed solids has shown that already very small displacements  $\Delta x$  in the order of  $d_{nucl} \approx 0.2 \cdot 10^{-10}m$  lead to high decay rates in the order of  $10^9 s^{-1}$ . The investigation of concrete detectors in the next chapter will show that physical processes accompanying the detection process, as e.g. changing electric fields etc., can easily cause displacements of this order and even much bigger ones. Therefore, if there is no perfect synchronization in time, the quantum superposition is broken stepwise, where one has at each step only the concurrency of two states, for which the projection postulate is exactly reproduced.

Another point is that the ratio between the detection probabilities of the two detectors does not show any deviations from the projection postulate. Only the absolute values of the reduction probabilities are different. But this difference is small, if the detection zones of the detectors are small compared to the extension of the particle.

In the discussion of further types of experiments one should keep in mind that not only the detection processes inside the detector, but also its interaction with the environment causes small displacements of solids. To be specific, this can be the interaction with the detector's power supply or with the device storing finally the measurement result, as indicated for the upper detector of experiment c) (Figure 5). Therefore the discussion, whether the result of an experiment is consistent to the proposed model or not, requires a detailed analysis of all processes accompanying the detection process. Normally, experimentalists do not care about these processes, which makes a subsequent discussion of experiments difficult. More clarity, whether the proposed reduction model is correct, can only be achieved by experiments, in which all processes accompanying the detection process are carefully controlled. Such an experiment is proposed in the following chapter.

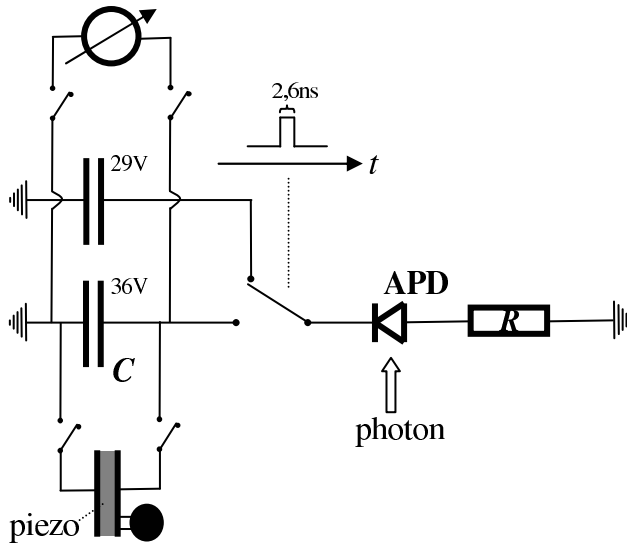


**Fig. 6** Proposed circuit for the detectors of the thought experiments of Figures 3a and 3b. If the piezo control at the bottom is connected by the two switches, the detector is operating in the MDD changing mode, otherwise in the MDD conserving mode.

#### 4 Proposed experiment

In this chapter the question is discussed to what extent it is possible to verify the predictions of the model with current state of the art technology. This is done by proposing and investigating a concrete realization for the thought experiments of Figure 3a and 3b. Figure 6 shows the proposed circuit for the photon detector, which can be operated in the MDD conserving and MDD changing mode as well: If the piezo at the bottom is connected by the two switches to the circuit, the detector is operating in the MDD changing mode, otherwise in the MDD conserving mode. An important strategy of the proposed reduction experiment is that the reduction process itself is part of the experiment and is not induced by an external observation process. This is realized as follows. The information about the photon measurement will be stored during the detection process inside the detector and will not be forwarded to an external observer. Sufficient time after the reduction event has taken place the observer can read out the measurement result from the detector. In the circuit of Figure 6 the photon detection leads to a voltage drop in the lower capacitor, which can be measured afterwards by connecting the voltage meter to the capacitor with help of the two switches. The photon detection is realized by an avalanche photodiode (APD), which is biased above its breakdown voltage. At this so-called Geiger mode a single photon can generate - by exciting an electron hole pair - an avalanche, which leads to a macroscopic current pulse. In the experiment two characteristics of the APD are important:

1. The quantum efficiency, which is the probability to detect the photon.

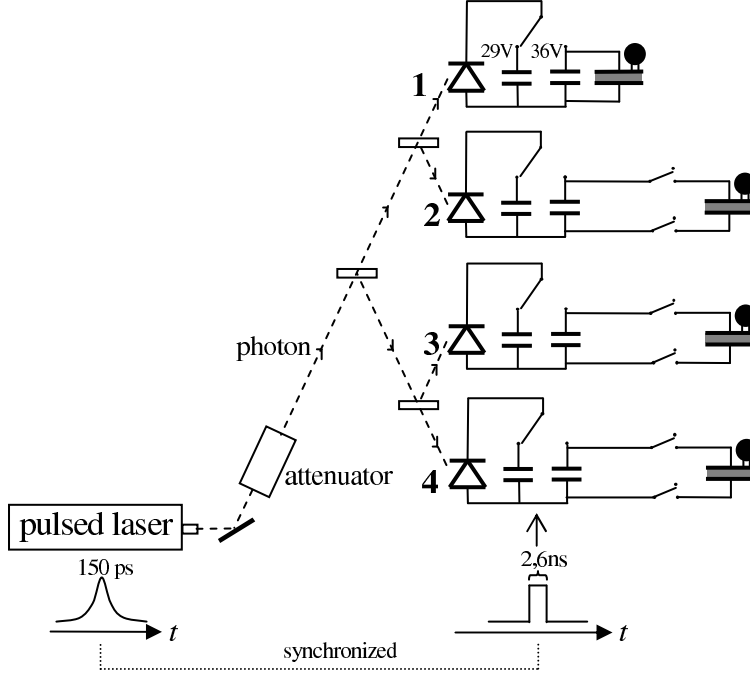


**Fig. 7** Complete experimental setup of the proposed experiment. The setup allows to toggle by connecting/disconnecting the piezos for the three lower detectors between the thought experiments of Figures 3a and 3b.

2. The dark count probability, which is the probability to measure a photon without a stimulating photon.

The dark count probability can be reduced significantly by operating the APD in the so-called gated mode [24]. Here the bias voltage will be kept slightly below the breakdown voltage and raised above the breakdown level only inside a window, at which the photon is expected. Quantum efficiency and dark count probability increase both with the voltage at the APD. They can therefore not be adapted independently from each other. For an InGaAs/InP APD cooled to 77 K combinations of 60% and  $10^{-4}$  (quantum efficiency, dark count probability) or 10% and  $10^{-6}$  are possible [24]. The circuit of Figure 6 works now as follows. At the beginning of the measurement the capacitors will be charged to 36 V and 29 V respectively, where 29 V is below and 36 V above the breakdown voltage of InGaAs/InP at 77 K [24]. The switch connects the APD with the upper capacitor. At the time, where the photon is expected, the switch changes to the lower capacitor of 36 V within a time window of 26 ns (see Figure 6). If the photon triggers an avalanche, the voltage of the lower capacitor will decrease due to the avalanche current, which will stop after some time. In the MDD changing mode the voltage drop in the lower capacitor affects also the connected piezo, which in turn shifts the position of the connected rigid mass. A MDD changing detector using an APD and a piezo for shifting a mass was already realized and used in another context [25].

Figure 7 shows the complete experimental setup, which allows to toggle between the experiments of Figure 3a and 3b, by connecting/disconnecting the piezos of the three lower detectors. The single photons are generated by short laser pulses of 150 ps, which are attenuated by 100 db [24]. For the InGaAs/InP APDs a photon wavelengths in the infra red of  $\lambda = 1.3 \mu\text{m}$  is needed [24]. The probability that the laser emits exactly one photon (single photon efficiency) depends on the attenuation. Cases, where no photon or more than one photon are emitted, can be eliminated from the measurement series by evaluating the detection results of all four detectors. The switch for the 2.6 ns gate is synchronized with the laser pulse (see Figure 7). To eliminate long-term drifts in the comparison of the experiments of Figure 3a and 3b, as e.g. changes of quantum efficiencies of the APDs or drifting mirror alignments, one can toggle between both configurations by connecting/disconnecting the piezo controls of the three lower detectors at every second measurement. The accuracy with which the reduction probability  $p_1$  for Detector 1 can be measured depends on the number of measurements like  $\Delta p_1 \approx 1.3 \cdot N_{succ}^{-1/2}$ , where

$N_{succ}$  denotes the number of successful measurements, at which exactly one photon was detected in one of the four detectors. To achieve with a quantum efficiency of the APD of 50% an accuracy of  $\Delta p_1 = 10^{-2}$ , one needs roughly  $3 \cdot 10^4$  measurements.

The proposed experiment is facilitated by the fact that one has not to care about the coherence of the superposed quantum states since the predicted deviations from the projection postulate are not expected to be sensitive to decoherence (see Chapter 2). In the proposed experiment the trigger rates (5) become significant, when the piezo starts to move the mass. Here the coherence between the four superposed states is already lost mainly due to the avalanche currents in the detectors.

We turn now to the decisive question, whether the proposed circuit of Figure 6 can be designed in such a way that it satisfies approximately the requirements of a MDD conserving detector. The decay rate of the MDD conserving detector  $E_{G con}/\hbar$  which is given by  $E_{G i,j}$  between the states "photon detected" and "no photon detected" has to be significantly lower than the decay rate  $E_{G cha}$  of the MDD changing detector ( $E_{G con}/E_{G cha} \ll 1$ ). From the discussion in Chapter 3 it follows that a decay rate of the MDD changing detector in the order of  $E_{G cha}/\hbar \approx 10^9 s^{-1}$  can easily be achieved. Several physical effects contribute to the decay rate of the MDD conserving detector. The following effects are only a selection:

1. One effect occurring in the capacitor  $C$  of the circuit of Figure 6 is the compression of its dielectric, which changes slightly due to the voltage drop by the avalanche current. Assuming that the avalanche current causes a voltage drop from 36 to 29 V one gets for a circular plate capacitor with radius  $r=5$  cm, a plate distance of  $d=0.1$  mm and  $\text{SiO}_2$  as dielectric ( $\epsilon \approx 3.7$ , compression module  $E \approx 7.6 \cdot 10^{10} \text{ Nm}^{-2}$ ), which corresponds to a capacity of  $C \approx 2.6$  nF, a change of the plate distance of roughly  $\Delta d \approx 2 \cdot 10^{-15}$  m, which is 10.000 times smaller than the extension of the nuclei  $d_{nucl} \approx 0.2 \cdot 10^{-10}$  m. With equation (18) the contribution of this effect to  $E_{G con}$  can be estimated as  $E_{G con}/\hbar \approx 10^{-15} s^{-1}$ .
2. A further effect occurring in the capacitor is due to the changing numbers of electrons on its plates by the avalanche current, which leads to a small change of the mass density of the plates due to the electron's masses. The contribution of this effect to  $E_{G con}$  can be estimated with equation (1) as  $E_{G con}/\hbar \approx 10^{-15} s^{-1}$ .
3. An effect occurring in the resistor  $R$  of the circuit of Figure 6 is its heating by the avalanche current, which leads via thermal extension to small displacements of the resistor. Assuming that the resistor is just a wire of Cu (extension coefficient  $\alpha \approx 1.7 \cdot 10^{-5} \text{ K}^{-1}$ ) with length  $l=10$  cm and diameter  $d=3$  mm, which corresponds to a resistance of  $R \approx 2.4 \cdot 10^{-4} \Omega$ , one gets for a discharge of the capacitor ( $C \approx 2.6$  nF) from 36 to 29 V a change in the resistor's length of  $\Delta l \approx 4 \cdot 10^{-13}$  m, which is 50 times smaller than  $d_{nucl} \approx 0.2 \cdot 10^{-10}$  m. With equation (18) the contribution of this effect to  $E_{G con}$  leads to a decay rate of  $E_{G con}/\hbar \approx 10^5 s^{-1}$ .
4. A further effect is caused by the impetus of the photon, which transmits its impetus to the detector, leading to a small movement of the detector and a displacement  $\Delta x$  increasing linearly with time. The contribution of this effect to  $E_{G con}$  is after one second still smaller than  $E_{G con}/\hbar \approx 10^{-20} s^{-1}$ .

This first analysis is encouraging since the strongest effect the heating of the resistor is with a decay rate of  $E_{G con}/\hbar \approx 10^5 s^{-1}$  still 10,000 times smaller than the assumed decay rate of the MDD changing detector  $E_{G cha}/\hbar \approx 10^9 s^{-1}$ . But nevertheless, a lot of further challenges remain to keep the detector's decay rate sufficient small, as e.g. the engineering of the five electronic switches in the circuit of Figure 6 or to keep the environments contribution to the decay rate of the detector as small as possible.

Another aspect for the dimensioning of the experiment is that the lifetime of the MDD conserving detector (here  $\tau_{con} \approx 10 \mu s$ ) has to be significantly bigger than fluctuations in the reaction times of the APDs, which can be defined by the time span between the entering of the photon into the APD and the point in time, at which the avalanche current has reached a certain strength. Measurements of such fluctuations are not known by the author and should be checked for the chosen APDs.

An issue which will remain open in this work is the question how far the macroscopic quantum states have to be separated from each other in configuration space so that they can be regarded as separated states in terms of the proposed model and how their separation can be defined. This issue can be explained with help of the experiment shown in Figure 8, at which the three MDD conserving

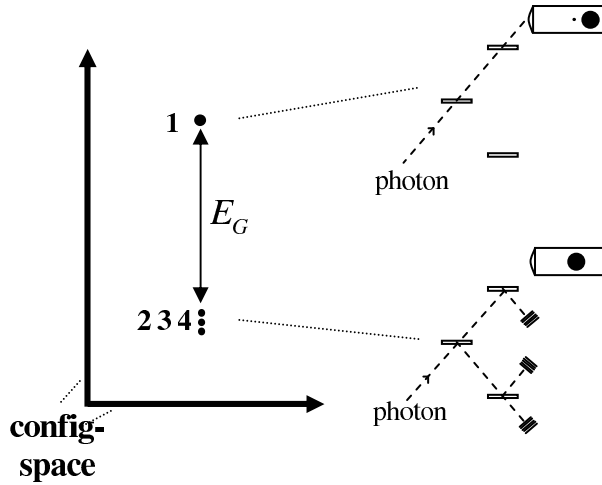


**Fig. 8** Modification of the experiment of Figure 3b, at which the states 2, 3 and 4 converge so close in configuration space that they can be treated as one state, as shown at the left part of the figure.

detectors of the experiment of Figure 3b are removed. This experiment resembles the one of Figure 2. The only difference is that the photon is distributed at three concrete locations instead blurred around the detector. The states 2, 3 and 4 are now so close in configuration space that they can be treated as one state (see Figure 8). For the matrix  $E_{G_{i,j}}$  one has therefore to regard only the concurrency of two states leading to the reduction probabilities of the projection postulate. Hence there has to be a smooth transition of the reduction probabilities of the experiment of Figure 8 towards the ones of the experiment of Figure 3b depending on the separation of the states. A possible criterion for this separation could be the number of particles participating at the photon detection process combined with the distance the particles are moving at the detection process. For the proposed experiment it is assumed that the electrons moving with the avalanche current from one side of the capacitor to the other cause a sufficient separation of the states.

To sum up, the analysis of the experimental proposal has shown that a verification of the predicted effects should be possible with current state of the art technology.

## 5 Outlook to biology

Encouraged by the fact that the reduction behavior of the model is not expected to be sensitive to decoherence the question shall be investigated whether the predictions of the model can play a role in biology. This investigation is additional motivated by the matter of fact that the Diósi-Penrose hypothesis predicts longer life-times for quantum superpositions in an fluid environment (as e.g. in a cell) than for quantum superpositions of solids, which can be explained as follows. Since the particles in a fluid environment will move according to the Brownian motion, their wave-function will disperse and be blurred after some time. Consequently the microscopic mass-density distribution will become almost flat and will not have the sharp peaks as in solid states. Therefore the microscopic contribution to the decay rates of solid states  $E_{G_{nucl}} \cdot N_{nucl}$  (see Figure 4), which has its origin in the fact that the nuclei of the superposed states have to be separated from each other, plays no role, which should result in bigger lifetimes than in solids.

According to the discussion in Chapter 2 the most significant deviation from the projection postulate is expected for a superposition of many states, from which only one state is distinguished by a different mass-density distribution. In the following it will be shown that a cell, e.g. a bacterium, can evolve in such a quantum superposition. According to the Löwdin two-step model for mutations the modification of a DNA molecule is initiated by a quantum tunneling process of an H-bounded proton between two adjacent sites within a base pair [26] leading to the generation of a tautomeric form of a DNA base

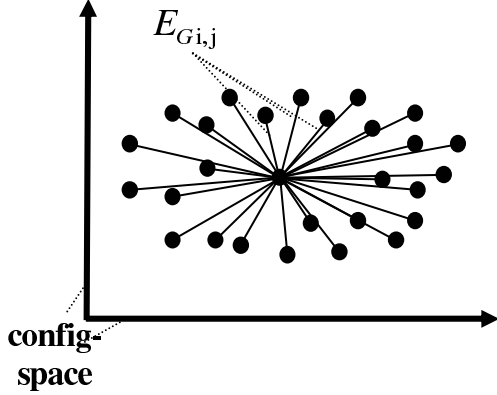


**Fig. 9** Visualization of the matrix elements  $E_{Gi,j}$  for a set of superposed states in a cell by connecting lines between the states. The state in the centre distinguishes from all others by its mass-density distribution due to the catalysis of a chemical reaction.

(e.g. keto guanine  $\rightarrow$  enol guanine). In the second step the tautomeric DNA base can lead at the replication of the DNA strand to an incorporation of an incorrect base (e.g. enol guanine with keto thymine instead of cytosine). After the tunneling of the proton the wave-function of the whole cell consists of two superposed states, which differ from each other by only one base pair in one DNA molecule. But the superposed states will differ much more from each other, when the cells starts to replicate the DNA molecule and to produce proteins from it in its ribosomes. According to the Diósi-Penrose hypothesis the superposition of the cell is at this stage far from the point where a reduction is expected. Note that the evaluation of  $E_{G1,2}$  for a superposed sphere of water with a diameter of  $1\mu\text{m}$ , where the two superposed states are separated far from each other, leads to a life-time in the order of seconds. Since bacteria have extensions of this order, the stability of the superposition is expected to be orders of magnitude above this time scale. The stability of the superposition can reduce significantly, if the protein produced in one of the states is an enzyme that enables the cell to live from a chemical substance (e.g. lactose) available in its environment. This will lead to metabolism between the cell and its environment, which in turn causes movement of masses and therefore leads to a change of the mass-density distribution. If one assumes that the proton tunneling occurs with a small probability and with a constant rate for all sections of the DNA molecule, the amplitude corresponding to the original DNA molecule  $|c_1|^2$  will decrease slightly at each proton tunneling. Assuming that the amplitudes of the separated states with the modified DNA molecules have all the same amount, their amplitudes are given by  $|c_i|^2 = (1 - |c_1|^2)/n$ , where  $n$  is the number of occurred proton tunnelings. All the states of the superposition will correspond to different types of produced enzymes, where normally only the state with the original DNA molecule will be able to catalyze the chemical substance available in the environment. The matrix  $E_{Gi,j}$  for the superposed states in the cell is visualized in Figure 9 by connecting lines between the states. Since only state 1 with the original DNA molecule leads to metabolism and therefore to a change of the mass-density distribution, all matrix elements are vanishing except the ones between this and all other states. These matrix elements have all the same amount. From equation (13) follows that the reduction probability of the superposition towards the original state 1 is given by

$$p_1 \approx 1 - \frac{1}{n} \cdot \frac{1 - |c_1|^1}{|c_1|^2}, \quad (20)$$

which means that the probability for the superposition to reduce back to the original "good state" (i.e. the state, which enables the cell to live from the food of its environment) is almost 100% for big  $n$ , even if the amplitude  $|c_1|^2$  has reduced significantly.

The derived model could be suitable to explain the effect of adaptive mutation first observed on *Escherichia coli* bacteria [27]. A non-fermenting strain of *Escherichia coli* bacteria, which means that this mutant of *Escherichia coli* is not able to live from lactose, shows a significant increased mutation rate of its DNA molecules towards a lactose-fermenting mutant, if one changes the food on its agar plate

to lactose only. This mutation effect occurs on non-growing strains, i.e. the bacteria do not replicate themselves during the mutation [27]. Some attempts were already made to explain this phenomenon by quantum mechanical effects [28, 29, 30]. With the derived reduction model the explanation of adaptive mutation could be as follows. If the food on the agar plate of the bacteria strain is changed to lactose, the state with the unmodified DNA molecule will not lead to metabolism and consequently to a change of the mass-density distribution anymore. Instead the state with the lactose-fermenting mutant will be distinguished from all other states. From equation (13) it follows that the reduction probability towards this state is given for big  $n$  by

$$p_i \approx \frac{1 - |c_1|^1}{2 - |c_1|^2}, \quad (21)$$

which leads to a significant non-vanishing probability towards this state, which is for big  $n$  orders of magnitudes bigger than the probability expected from the projection postulate  $p_i = |c_i|^2$ . This behaviour might be nominated as "selective reduction" since the state that is the best for the survival of the cell gets a strong increased reduction probability. Further ideas, how selective reduction can play a role in biology, were published by the author in reference [31].

## 6 Discussion

The following discussion deals the following two issues. First, it is attempted to define an generalized experimental agenda, which is independent from the specific approach of the phenomenological model and the assumption that the physical couplings are governed by gravity. It shall base only on the thesis that quantum state reduction has its origin in a mutual physical interaction between the states. Second, the approach is analyzed from the view point of quantum non-locality in concrete its consequences for signaling.

A conclusion, which can be extracted from the analysis of the phenomenological model is that changes of the strengths of the physical couplings between the states should lead to somehow changes of the reduction probabilities. An experimental agenda verifying this thesis would be characterized at least by the following points:

1. Superpositions of more than two states have to be investigated (otherwise condition 2 can't be fulfilled).
2. The coupling strengths between the states have to be chosen significantly different. It is recommended to compare reduction probabilities of experiments with equal and significantly different coupling strengths as proposed in Figure 3. Beneath gravity-induced quantum state reduction other theses for the physical origin of the couplings  $E_{G i,j}$  or modifications of the Diósi-Penrose approach should be tested<sup>6</sup>.
3. The different coupling strengths become relevant in a regime, where the states have already lost their coherence to each other.

Experiments fulfilling these conditions were not performed so far. It is evident to mention that the proposed program should also check for smaller changes of reduction probabilities than predicted by the model. This requires long measurement times, since the accuracy of probability measurements  $\Delta p$  scales with the number of returns  $N$  like  $\Delta p \approx N^{-1/2}$ .

Point 3 of the agenda might look for many physicists unusual. Normally it is not expected that quantum effects are further relevant when the states have lost their coherence to each other. Point 3 can simply be justified from the experimental fact that it was so far not possible to observe state reduction at a quantum interference experiment. Therefore state reduction has to take place in a regime, where

<sup>6</sup> In this context it is interesting to mention that with the assumption that state reduction by a physical interaction between the states leads to changed reduction probabilities it is possible to determine the coupling strengths  $E_{G i,j}$  by a modification of the proposed experiments. This requires to change the MDD conserving detectors of experiment 3b in the way that they move a rigid mass like the MDD changing detectors but with a time delay  $\Delta t$  after the photon has entered the detector. This delayed change of the mass-density distribution can impact the measurements result only if the four states are still in a superposition. By measuring changes of the reduction probabilities of experiment 3b and the modified experiment as function of the time delay  $\Delta t$  it is possible to determine the superposition's life-time and accordingly the coupling strengths.

quantum coherence between the states is already lost. As already stated the phenomenological model predicts also no dependence of the reduction probabilities from the coherence between the states. They depend only on the amplitudes of the states (see equation 13). At the proposed experiment in Chapter 4 the four superposed states have also lost their coherence when the rigid mass inside the detectors is moved mainly due to the avalanche currents in the APDs.

A question of general concern is whether quantum state reduction by a mutual physical interaction between the states activates signalling via quantum non-locality. From the conclusion that this thesis leads to deviant behavior from the projection postulate one can easily construct experiments which enable signaling via quantum non-locality. This shall be exemplarily shown by a modification of the thought experiment of Figure 3. By removing the upper detector in Figure 3 spatial far from the three lower ones, information can be exchanged between the two locations by changing the modes of the three lower detectors between MDD changing and MDD conserving. By estimating several measurements in the upper detector the mode of the three lower detectors can be determined via the changed reduction probabilities for the upper detector. Since Bell-type experiments demonstrate faster-than-light correlations of separated measurements via quantum non-locality of state reduction [2] it is very likely that the proposed experiment leads to faster-than-light signaling, since the exchange of information bases on state reduction. If one interprets the state amplitudes of the phenomenological model  $|c_i|$  as global properties of the system and assumes that these amplitudes change abruptly when the decay of the superposition is triggered, one comes to the same conclusion. This does not change if one takes into account that the state amplitudes  $|c_i|$  might not change abruptly but with a somehow time-dependency. Also the experiments restriction that one can not forward the detector's results instantaneously to an observer but has to wait until the superposition is decayed completely before reading out the detector's result does not change the conclusion.

This provokes the question whether the thesis contradicts to existing proves for the impossibility of superluminal signaling. These proves investigate the question whether a measurement on a quantum state can influence the result of an other spatially far separated measurement [32]. The impossibility of an influence on the second measurement bases on the fact that the measurement operators of the spatially separated measurements commute with each other [32]. These proves can not be applied to the proposed experiments of this work. Here one has not a sequence of two measurements corresponding to two separated state reductions but a single spatially distributed measurement.

The conflict of the supposed thesis with superluminal signaling comes from the conclusion that a mutual physical interaction between the states allows to change the reduction probabilities. This means that it is possible to control global properties of the system (the state amplitudes  $c_i$ ) and to use quantum non-locality for the exchange of information. Therefore any deviation from the projection postulate and even it is very small will be of big importance for the question of faster-than-light signaling. From this point of view the proposed experimental agenda could alternatively also be regarded as a test for the general validity of the projection postulate and the impossibility of faster-than-light signaling.

To sum up, a careful execution of the proposed experimental program, characterized by the above three issues, which checks reduction probabilities also for small deviations from the projection postulate and tests beneath the gravitational hypothesis further hypotheses for the physical couplings, will give us a deeper insight into the nature of quantum state reduction. A negative result would manifest the projection postulate as a fundamental principle of nature and confirm the impossibility of superluminal signaling. It would be a clear hint against the thesis that quantum state reduction has its origin in a physical interaction between the superposed states and show that state reduction is governed by other principles. A positive result would reveal a new aspect of quantum state reduction and would strongly stimulate further experimental and theoretical research.

## A Appendix: Derivation of equations 1 and 2 for the decay rate of a superposition

Equations 1 and 2 for the decay rate of a superposition can be derived with Penrose's argument that the time-translation operator of the superposition is ill-defined as follows. The component  $g_{00}$  of the metric tensor is given in the Newtonian limit by

$$g_{00} = 1 + \frac{2\phi(\mathbf{x})}{c^2}, \quad (22)$$



where  $\phi(\mathbf{x})$  is the gravitational potential. The derivation of the physical time  $\tau$  to the time coordinate  $t$  ( $c \cdot t = x_0$ ) is given by

$$\frac{d\tau}{dt} = \frac{ds}{dx_0} = \sqrt{g_{00}} \approx 1 + \frac{\phi(\mathbf{x})}{c^2}, \quad (23)$$

where  $s$  is the space-time invariant ( $ds = c \cdot d\tau$ ). The fuzziness of the energy of state 1 by due to the difference of the time-translation operators of state 1 and 2 can be estimated by

$$\Delta E_1 = \int d^3\mathbf{x} \rho_1(\mathbf{x}) c^2 \left( \frac{d\tau_2}{dt} - \frac{d\tau_1}{dt} \right) = \int d^3\mathbf{x} \rho_1(\mathbf{x}) (\phi_2(\mathbf{x}) - \phi_1(\mathbf{x})) \quad (24)$$

and for state 2 analogous

$$\Delta E_2 = \int d^3\mathbf{x} \rho_2(\mathbf{x}) c^2 \left( \frac{d\tau_1}{dt} - \frac{d\tau_2}{dt} \right) = \int d^3\mathbf{x} \rho_2(\mathbf{x}) (\phi_1(\mathbf{x}) - \phi_2(\mathbf{x})). \quad (25)$$

The addition of  $\Delta E_1$  and  $\Delta E_2$  leads directly to expression 1 for  $E_{G1,2}$ :

$$\Delta E_1 + \Delta E_2 = \int d^3\mathbf{x} (\rho_1(\mathbf{x}) - \rho_2(\mathbf{x})) (\phi_2(\mathbf{x}) - \phi_1(\mathbf{x})) = G \int d^3\mathbf{x} d^3\mathbf{y} \frac{(\rho_1(\mathbf{x}) - \rho_2(\mathbf{x}))(\rho_1(\mathbf{y}) - \rho_2(\mathbf{y}))}{|\mathbf{x} - \mathbf{y}|} = E_{G1,2}. \quad (26)$$

The corresponding frequency of the energy fuzziness  $\nu = (\Delta E_1 + \Delta E_2)/\hbar$  yields the decay rate  $\dot{p}_{decay}$  of equation 2.

**Acknowledgements** I thank Prof. Wolfgang Elsässer for valuable support at the design of the proposed experiment. I thank Prof. Werner Martienssen, Prof. Gernot Alber, Dr. Eric Hildebrandt, Dr. Helmar Becker, Prof. Wolfgang Dultz, Prof. Achim Richter and Prof. Thomas Görnitz for interesting and helpful discussions. I thank Dr. Christoph Lamm for proofreading the manuscript. This work is dedicated to my parents.

## References

1. J. von Neumann, Mathematical Foundations of Quantum Mechanics, Princeton University Press, Princeton (1955)
2. D. Salart, A. Baas, J. C. Branciard, N. Gisin, H. Zbinden, Testing spooky action at a distance, *Nature*, 454, 861 (2008)
3. M. Arndt, O. Nairz, J. Voss-Andreae, C. Keller, G. van der Zouw, A. Zeilinger, Wave-particle duality of C60 molecules, *Nature*, 401, 680-682 (1999)
4. J. Friedman, V. Patel, W. Chen, S. Tolpygo, J. Lukens, Quantum superposition of distinct macroscopic states, *Nature*, 406, 43-46 (2000)
5. G.J. Milburn, Intrinsic decoherence in quantum mechanics, *Phys. Rev. A*, 44, 5401-5406 (1991)
6. L. Diósi, Models for universal reduction of macroscopic quantum fluctuations, *Phys. Rev. A*, 40, 1165-1174 (1989)
7. R. Penrose, On gravity's role in quantum state reduction, *Gen. Rel. Grav.*, 28, 581-600 (1996)
8. G. C. Ghirardi, A. Rimini, T. Weber, Unified dynamics for microscopic and macroscopic systems, *Phys. Rev. D*, 34, 470 (1986)
9. G. C. Ghirardi, P. Pearle, A. Rimini, Markov processes in Hilbert space and continuous spontaneous localization of systems of identical particles, *Phys. Rev. A*, 42, 78-89 (1990)
10. W. Marshall, C. Simon, R. Penrose, D. Bouwmeester, Towards quantum superpositions of a mirror, *Phys. Rev. Lett.*, 91, 130401 (2003)
11. J. Christian, Testing gravity-driven collapse of the wavefunction via cosmogenic neutrinos, *Phys. Rev. Lett.*, 95, 160403 (2005)
12. R. Penrose, Quantum computation, entanglement and state reduction, *Trans. R. Soc. Lond. A*, 356, 1927-1939 (1998)
13. J. van Wezel, T. Oosterkamp, J. Zaanen, Towards an experimental test of gravity-induced quantum state reduction, arXiv:0706.3976v1, 5 Feb. (2008)
14. F. Károlyházi, A. Frenkel, B. Lukács, Physics as natural philosophy, MIT, Cambridge MA (1982)
15. P. Pearle, E. Squires, Bound state excitation, nucleon decay experiments, and models of wave function collapse, *Phys. Rev. Lett.*, 73, 1-5 (1994)
16. B. Lamine, M. T. Jaekel, S. Reynaud, Gravitational decoherence of atomic interferometers, *Eur. Phys. J. D*, 20, 165-176 (2002)
17. W. L. Power, I. Percival, Decoherence of quantum wave packets due to interaction with conformal space-time fluctuations, *Proc. Roy. Soc. Lond. A*, 456, 955-968 (2000)
18. S. Bose, K. Jacobs, P. L. Knight, Scheme to probe the decoherence of a macroscopic object, *Phys. Rev. A*, 59, 3204-3210 (1999)
19. C. Henkel, M. Nest, P. Domokos, R. Folman, Optical discrimination between spatial decoherence and thermalization of a massive object, *Phys. Rev. A*, 70, 023810 (2004)

- 
20. C. Simon, D. Jaksch, Possibility of observing energy decoherence due to quantum gravity, *Phys. Rev. A*, 70, 052104 (2004)
  21. G. Amelino-Camelia, Gravity-wave interferometers as probes of a low-energy effective quantum gravity, *Phys. Rev. D*, 62, 024015 (2000)
  22. R. Penrose, *Shadows of the mind: an approach to the missing science of consciousness*, Oxford University Press, Oxford (1994)
  23. L. Diósi, Intrinsic time-uncertainties and decoherence: comparison of 4 models, *Brazilian Journal of Physics*, 35, 260-265 (2005)
  24. G. Ribordy, J.D. Gautier, H. Zbinden, N. Gisin, Performance of InGaAs/InP avalanche photodiodes as gated-mode photon counters, *Applied Optics*, 37, 2272-2277 (1998)
  25. D. Salart, A. Baas, J. A.W. van Houwelingen, N. Gisin, H. Zbinden, Spacelike Separation in a Bell Test Assuming Gravitationally Induced Collapses, *Phys. Rev. Lett.*, 100, 220404 (2008)
  26. P.O. Löwdin, *Advances in Quantum Chemistry*, 213-360. Academic Press, New York (1965)
  27. J. Cairns, J. Overbaugh, S. Millar, The origin of mutants, *Nature*, 335, 142-145 (1988)
  28. J. McFadden, J. Al-Khalili, A quantum mechanical model of adaptive mutation, *Biosystems*, 50, 203-211 (1999)
  29. A. Goswami, D. Todd, Is there conscious choice in directed mutation, phenocopies, and related phenomena?, *Integr. Physiol. Behav. Sci.*, 32, 132-142 (1997)
  30. V.V. Ogryzko, A quantum-theoretical approach to the phenomena of directed mutations in bacteria (hypothesis), *Biosystems*, 43, 83-95 (1997)
  31. G. Quandt-Wiese, *Evolutionary Quantum Theory and the Physical Representation of Awareness*, Mensch & Buch Verlag, Berlin (2002)
  32. G. C. Ghirardi, A General Argument against Superluminal Transmission through the Quantum Mechanical Measurement Process, *Lettere al Nuovo Cimento*, 27, page 293 (1980)